SAR Processing of Ground-Penetrating Radar Data for Buried UXO Detection: Results from a Surface-Based System

Jennifer I. Halman, Keith A. Shubert, *Member, IEEE*, and George T. Ruck

***Abstract*— Battelle and The Ohio State University ElectroScience Laboratory have built and demonstrated a ground-penetrating radar (GPR) system for locating buried unexploded ordnance (UXO). The system is ground based and towed by an autonomously controlled vehicle as part of the Subsurface Ordnance Characterization System (SOCS). This paper presents the results of the synthetic aperture radar (SAR) processing of the radar data acquired at Tyndall Air Force Base, FL, and Jefferson Proving Ground (JPG), IN. A companion paper by Chen and Peters presents the results of the complex natural-resonance processing used to identify the size of the ordnance items.**

***Index Terms*— Buried object detection, synthetic aperture radar.**

I. Introduction

BATTELLE and The Ohio State University ElectroScience Laboratory (ESL) have built and demonstrated a ground penetrating radar (GPR) system for locating buried unexploded ordnance (UXO). The system is ground based and towed by an autonomously controlled vehicle as part of the Subsurface Ordnance Characterization System (SOCS). The system has been demonstrated at test areas at Tyndall Air Force Base, FL, and Jefferson Proving Ground (JPG), IN. Radar data from the SOCS GPR has been processed and will be presented. Synthetic aperture radar (SAR) processing was used to create an image of the area of interest indicating the target locations. A linear function was used to approximate the propagation velocity decreasing as a function of depth in the soil at JPG. Scientists at ESL have applied a complex natural resonance analysis technique to the SAR-detected targets to discriminate between buried UXO and clutter items [1].

Ground penetrating radar and SAR have been applied to buried UXO from both airborne [2] and ground [3] platforms by other authors.

II. SOCS Ground Penetrating Radar Description

The ground based GPR is a pulsed radar system with frequency content between 50 and 500 MHz. The radar and a pair of seven-foot cross bow tie dipole antennas are mounted with magnetometers on a nonferrous towed platform built by Battelle. A commercial impulse radar system, which transmits a 1-ns pulse, was used with the antenna designed and built by ESL. The antenna was designed to operate from 20 to 200 MHz. Wright Laboratories at Tyndall AFB developed the autonomous towing vehicle. The Wright Laboratories group, along with subcontractors, also developed the Simultaneous Data Collection and Processing System (SIDCAPS), which controls the autonomous vehicle and stores all of the sensor data. The position of the GPR antenna as a function of time is determined from position and heading information supplied by a global positioning system (GPS) on the tow vehicle and pitch, roll, and yaw sensors on the hitch.

Manuscript received January 21, 1997; revised September 25, 1997. This work was supported by the Naval Explosive Ordnance Disposal Technology Division and the U.S. Army Environmental Center.

The authors are with Battelle, Columbus, OH 43201 USA.

Publisher Item Identifier S 0018-926X(98)05779-2.

III. SAR Processing

In order to find buried UXO, the SOCS GPR is driven over the area of interest, collecting time-domain GPR data as it moves. Next, the SAR processing is performed, resulting in a three-dimensional (3-D) image that shows the locations of potential UXO as "bright spots." SAR processing of the time-domain GPR data consists of defining the volume to be imaged and constructing the SAR image. The time-domain GPR data are in the form of 256-point bipolar waveforms. The image is constructed by coherently summing (for each volume element in the image volume) the data point from each bipolar time-domain waveform that corresponds to the round-trip time between the GPR antenna and the volume element.

The data from the GPR antenna is in the form of an M by N two-dimensional integer array A. $A(m,n)$ is the nth data point in the mth received waveform. M is the number of waveforms recorded in the data set, which includes several parallel passes over the image area. N is the number of points in each waveform equal to 256. Δt is the time interval (equal to 0.5 ns) between data points in the GPR time-domain waveforms.

The 3-D SAR image is created by summing the appropriate data points from each waveform for each volume element in the image. To find the appropriate data points, we calculate the one-way distance d from the GPR antenna where it receives the mth waveform to the volume element. The volume element is centered at the coordinates (x,y,z). v is the velocity of propagation in the soil and the round-trip time t for the volume element is

$$t(m,x,y,z) = 2\frac{d(m,x,y,z)}{v}. \tag{1}$$

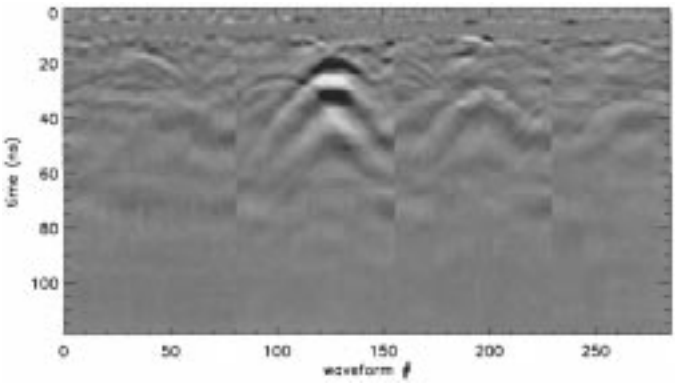

Fig. 1. Time-domain response of SOCS GPR to a target.

In the mth waveform, the time index n of A that contains the data from the volume element at (x, y, z) is

$$n(m, x, y, z) = \frac{t(m, x, y, z)}{\Delta t}. \tag{2}$$

The resulting 3-D SAR image sum for each volume element is $I(x, y, z)$ in (3).

$$I(x, y, z) = \sum_{m=0}^{M-1} A(m, n(m, x, y, z)). \tag{3}$$

Several factors are removed from the data array A before the summation in (3) is performed. Initially, the GPR waveforms include the antenna ringing, reflections from the surface and a gain slope of 30 dB. The antenna ringing is removed by subtracting an average waveform from each waveform and the gain slope is removed by multiplying each time waveform by a linear -30-dB gain-slope function. Fig. 1 shows an example of the time-domain GPR response to a target after subtraction of the average waveform and removal of the 30-dB gain slope. The targets appear as series of arcs. Four passes over the target are shown. The radar is nearest to the target in the second pass, where the response is the strongest. Before forming the SAR image, the time waveform is also shifted in time to place the beginning of the waveform at the surface of the ground.

The volume elements in the 3-D images presented in this paper are cubes, 20 cm on a side. The actual resolution of the image is difficult to quantify and needs to be determined experimentally. Several factors influence the cross-range resolution including bandwidth of the radar the size of the synthetic aperture, the antenna pattern, and factors associated with the properties of the soil. The SOCS antennas were designed to operate from 20 to 200 MHz, resulting in a down-range resolution of approximately 0.5 m. Losses in the soil and an increasing dielectric constant can effectively reduce the size of the aperture. Although the SOCS acquired data over an area of approximately 2500 m^2 and all of the data are available to create the synthetic aperture, the received waveform is only 128 ns long. In soil with a dielectric constant of 8.8, which is what we determined for Tyndall, a 128-ns waveform translates into a maximum one way distance of 6.5 m. We have found experimentally that an aperture with a radius of 3 m is useful, reducing the computation burden without noticeably degrading the resolution, at least for the data we have processed so far.

IV. Linear Approximation for the Soil Propagation Velocity

In general, the propagation velocity or dielectric constant of the soil is not uniform. The velocity may be a function of depth in the soil. Measurements of the dielectric constant and conductivity of the soil at the site at Tyndall Air Force Base indicate that the dielectric constant is approximately uniform at all depths with which the GPR is concerned. However, the measured dielectric constant of the soil at JPG is greater than at Tyndall and increases with depth. The loss tangent is also significantly higher. This condition complicates the calculation of the propagation time because the changing dielectric constant changes the velocity and also the path of the radar signal. The path becomes curved and the time it takes a signal to travel through the soil increases. The change is taken into account when doing the SAR processing with the following procedure.

If the dielectric constant is a function of depth z, the propagation velocity is some function $v(z)$. For a volume element at depth d and angle of incidence θ, geometrical optics and Snell's Law can be used to determine the path that connects the radar and a selected volume element. The radial distance r from the radar antenna is given by

$$r(d, \theta) = \int_0^d \sin\theta \frac{v(z)}{\sqrt{v_0^2 - v(z)^2 \sin^2\theta}}\, dz \tag{4}$$

for $0 \le \theta < \pi/2$. v_0 is the initial velocity in the soil at depth $z = 0$. The two-way propagation time is then

$$t(r, d) = \int_0^d \frac{2v_0}{v(z)\sqrt{v_0^2 - v(z)^2 \sin^2\theta}}\, dz. \tag{5}$$

However, when processing the GPR data, θ is not known. The depth of the volume element, d and the radial distance between the volume element and the radar r are known. Equation (4) is inverted to solve for θ. θ is substituted into (5) to find the two-way propagation time. If the velocity can be approximated as a linear function of the form

$$v(z) = v_0 - \alpha z \tag{6}$$

the integrals can be evaluated exactly.

$$r(d, \theta) = \frac{1}{\alpha \sin\theta} \times \left[\sqrt{v_0^2 - v_0^2 \sin^2\theta - \alpha^2 d^2 \sin^2\theta + 2v_0 \alpha d \sin^2\theta} - \sqrt{v_0^2 - v_0^2 \sin^2\theta}\right] \tag{7}$$

$$t(d, \theta) = \frac{2}{\alpha} \ln\left[\frac{v_0 + \sqrt{v_0^2 - v_0^2 \sin^2\theta - \alpha^2 d^2 \sin^2\theta + 2v_0 \alpha d \sin^2\theta}}{\sin\theta (v_0 - \alpha d)}\right] - \frac{2}{\alpha} \ln\left[\frac{v_0 + \sqrt{v_0^2 - v_0^2 \sin^2\theta}}{v_0 \sin\theta}\right]. \tag{8}$$

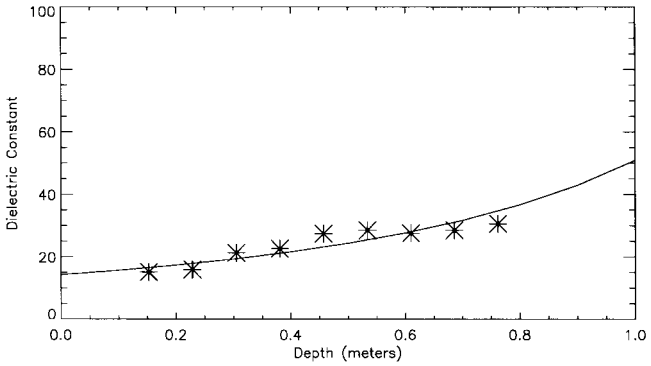

Fig. 2. Measured and approximated JPG soil dielectric constant.

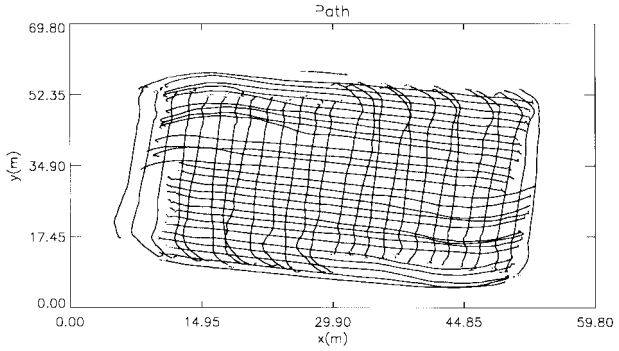

Fig. 3. SOCS GPR path at Tyndall.

To invert (7), for each volume element depth a vector containing the radial distances r_i is defined for the angles $\theta_i = (\pi/2)i/n$, where $n = 1000$. For each depth, r_i as a function of θ_i is known. To get θ as a function of r, an interpolation procedure is used that performs a linear interpolation on vectors with an irregular grid. This interpolation procedure gives θ_j for the known radial distances r_j and then the two-way time from (8).

ESL measured the dielectric constant at JPG near the test area as a function of depth. The measured dielectric constant and the dielectric constant function derived from the linear velocity function approximation used for the SAR processing are shown in Fig. 2.

V. SOCS GPR Results

A. Tyndall Results

Four complete GPR data sets were recorded at a test site at Tyndall Air Force Base. Known ordnance items were buried in sand at this site. The SOCS vehicle drove over the entire test pad four times, twice driving primarily north–south and twice driving east–west. The parallel passes were approximately 1.5–2.0 m apart. Fig. 3 shows the paths followed during one east–west run and one north–south run used to create the image in Fig. 4. Fig. 4 shows the SAR image collapsed to two dimensions. The image shown is the sum of the energy at all depths up to 3 m.

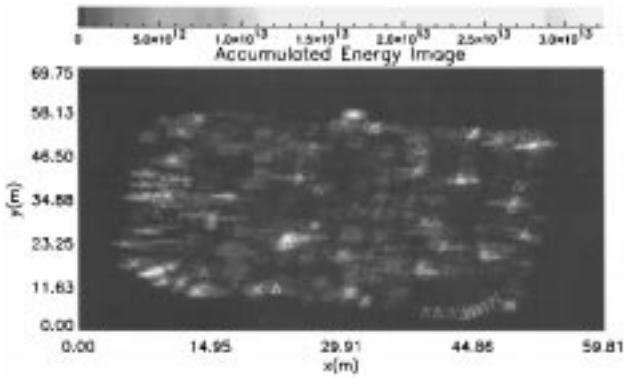

Fig. 4. Accumulated energy image at Tyndall.

In order to determine the coordinates of the ordnance items, we viewed images such as Fig. 4 and the entire 3-D SAR image. We visually located the center of the bright spots on slices of the 3-D image. The processing program allowed us to point and click on the center of the bright spot and recorded the coordinates of the spot selected. In the future, automatic thresholding may be added to the processing program.

Twenty-two pieces of ordnance and nine small plates were buried in known locations at Tyndall. The locations of the known targets are marked with triangles in Fig. 4. The SOCS path did not cover the area over the nine small plates, so we were not able to detect the plates. We found 17 of the 22 known buried ordnance items. The 17 ordnance locations are less than 2 m from one or more of the 38 potential target locations that we identified. The 38 potential target locations that we identified are shown with X's in Fig. 4. ESL used complex natural resonance (CNR) analysis to estimate the lengths of each target. In two instances, the CNR analysis revealed two resonances in a single location, indicating the possibility of multiple targets at those locations. We were not able to dig up the targets that we found in order to determine whether the locations of the known ordnance had shifted or the cause of the false alarms. There may have been other objects buried that caused the false alarms.

There were several problems encountered during the SOCS GPR Tyndall tests that should be corrected for future tests. One significant problem affecting the SAR imaging is an error in the recorded GPR antenna coordinates. The vehicle actually moved very smoothly, but the positions recorded by the system are not always evenly spaced. To correct for this, a 30-point running average was used on the coordinates of each trace. This process did improve the SAR image, however, there is still some possible position error, especially when the vehicle turns.

During all of the SOCS GPR Tyndall tests, the gain on the system was set too high. This resulted in a portion of the time waveform being clipped off. The time waveform was clipped off from 14.5 to 17.5 ns (5.75 to 8.75 ns after shifting the waveform in time to put the return from the surface at time zero). Due to the improper gain setting, the arcs in the time-domain data corresponding to shallow targets (those less than approximately 0.6 m deep) are incomplete or distorted, making it difficult to focus the shallow targets at the proper depth in

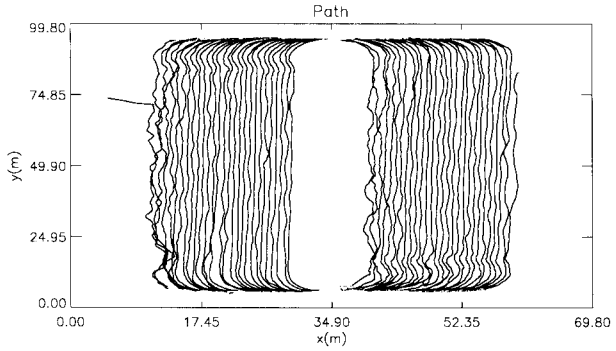

Fig. 5. SOCS GPR path at JPG area C22.

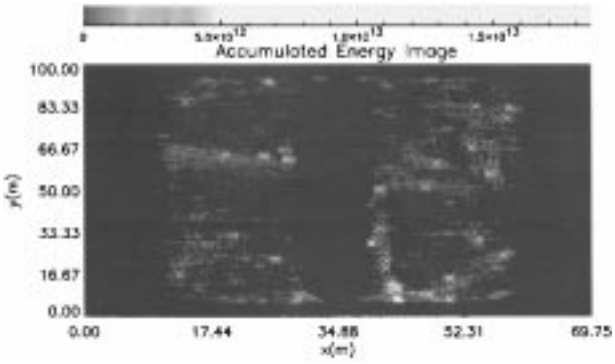

Fig. 6. Accumulated energy image for JPG area C22.

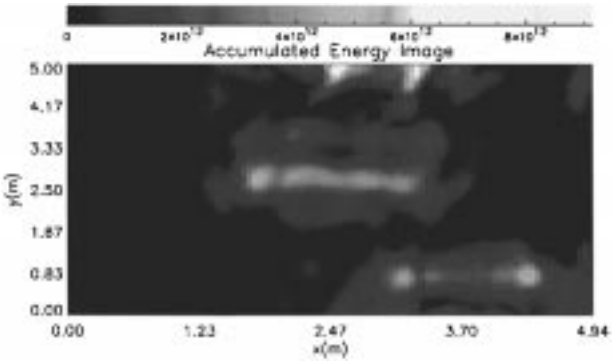

Fig. 7. Accumulated energy image using a uniform dielectric constant of 20 for a section at JPG.

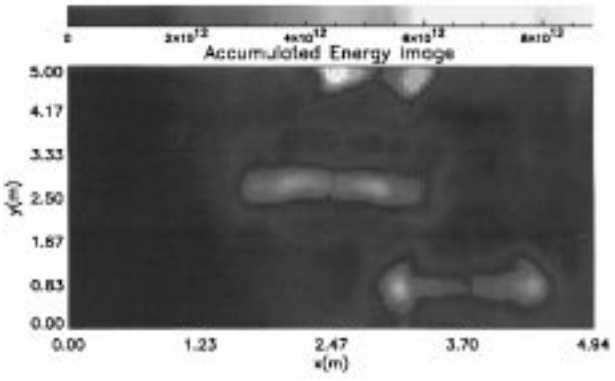

Fig. 8. Accumulated energy image using the approximation to the dielectric constant in Fig. 2 for a section at JPG.

the image. Some of the shallow targets are still detected from the resonances that appear deeper in the time-domain data.

Targets in the Tyndall images appear less focused in the direction perpendicular to the path. The data from two to three passes were processed for each volume element, but the targets would have appeared more focused in the direction perpendicular to the path of the vehicle if the passes were closer together so that more data points along the perpendicular direction could be included. During the SOCS Tyndall tests, the passes were 1.5–2 m apart. Adding the east–west and the north–south data sets improved the Tyndall resolution. During the JPG tests, the passes were less than a meter apart and the resolution improved.

B. JPG Results

One complete data set was obtained for an area at JPG. The path of the GPR antenna during the run is shown in Fig. 5. The parallel passes of the vehicle were designed to be 2.5 ft apart. Fig. 6 shows the accumulated energy image of the JPG data with the potential target locations marked, as determined from the SOCS GPR SAR image. CNR analysis was used to eliminate clutter and estimate the lengths of the targets. The true locations of the buried ordnance were not made available to Battelle or ESL.

The JPG data were processed both with the uniform propagation velocity and with a propagation velocity that decreases linearly with depth using the method described in this paper. The linear approximation is based on the measured dielectric constants of the soil at JPG. Fig. 7 shows the results for a small section of the test area using a uniform dielectric of 20. Fig. 8 shows the same section imaged using the linear approximation. The accumulated energy is for depths down to 1 m. The linear approximation does give a slightly better focused image of the target than the uniform dielectric approximation, but in both cases the target can be located.

VI. Conclusion

The SOCS GPR results are promising. Most of the buried ordnance items at Tyndall were located. Fewer targets were located at JPG with the SOCS GPR, but the soil conditions were much worse there. At Tyndall, the soil was relatively dry sand with a fairly uniform dielectric constant. The signal-to-noise ratio in the time-domain data was high enough to recognize targets. At JPG the soil was much lossier.

The SAR processing was very useful for identifying the locations of potential targets. The SAR images were used to create maps of the targets. Once the locations were identified, complex resonance analysis of the data from that location was used to determine whether or not a target existed and its approximate length.

Acknowledgment

The authors would like to thank C. C. Chen of the ElectroScience Laboratory, The Ohio State University, Columbus, for his assistance in working with the radar data.

REFERENCES

[1] C. C. Chen and L. Peters, "Buried unexploded ordnance identification via complex natural resonances," *IEEE Trans. Antennas Propagat.*, vol. 45, pp. 1645–1654, Nov. 1997.

[2] B. A. Safigan and R. L. Harris, "Real-time man-portable ground-penetrating synthetic aperture radar," in *UXO Forum Conf. Proc.*, Williamsburg, VA, Mar. 1996, pp. 357–361.

[3] C. F. Lee, J. K. Jao, D. J. Blejer, T. O. Grosch, S. Ayasli, S. M. Scarborough, E. M. Adams, K. Sturgess, and T. Ton, "Results and analysis of the 1995 Yuma ground penetrating radar experiment," in *UXO Forum Conf. Proc.*, Williamsburg, VA, Mar. 1996, pp. 405–414.

Jennifer I. Halman was born in Dayton, OH, on February 8, 1960. She received the B.S. (engineering physics) and M.S. (physics) degrees from The Ohio State University, Columbus, in 1982 and 1985, respectively.

In 1982, she joined Battelle, Columbus, OH, where she is now a Principal Research Scientist in the Electronics and Avionics Systems Department. She has participated in several ground penetrating radar programs, writing synthetic aperture radar processing software for ground-based and airborne ground-penetrating radar systems to find unexploded ordnance. Her research interests are electromagnetics, signal processing, and computer modeling. She is also interested in modeling and designing electromagnetic meshes and windows for electromagnetic interference shielding and other uses.

Keith A. Shubert (S'77–M'80) was born in Kansas City, MO, on November 22, 1951. He received the B.S.E.E., M.S., and Ph.D. degrees in 1974, 1975, and 1980, respectively, from The Ohio State University, Columbus.

From 1974 through 1980, he was a Graduate Research Associate at The Ohio State University ElectroScience Laboratory where he worked on low-frequency radar identification and discrimination techniques as well as periodic surface theory. Since 1981, he has worked at Battelle, Columbus, OH, where he has worked on numerous technical topics. Since 1992, he has headed the joint Battelle/ElectroScience Laboratory efforts in the areas of detection of buried unexploded ordnance and the detection of plastic antipersonnel land mines.

Dr. Shubert is a member of Eta Kappa Nu, Tau Beta Pi, and Sigma Xi. He is a former Chairman of the Columbus, OH, Joint Section of the IEEE Antennas and Propagation Society and Microwave Theory and Techniques Society.

George T. Ruck received the B.E.E. degree (electrical engineering) from The Ohio State University, Columbus, and the M.Sc. degree (electrical engineering) from the University of Washington, Seattle, in 1957 and 1960, respectively.

He has been with Battelle, Columbus, OH, since 1963. An authority in research related to electromagnetic theory and mathematical physics, he has conducted numerous studies related to advanced receivers, radar and electro-optical systems, electromagnetic and acoustic scattering from conducting, absorbing, and dielectric bodies, electronic warfare and camouflage materials, laser radar and communications, and navigation and precise positioning systems. He has authored or coauthored more than 175 reports and technical publications and is the editor and principal author of the two-volume book, *Radar Cross Section Handbook* (New York: Plenum, 1970).

Mr. Ruck is a member of the Society of Sigma Xi, Eta Kappa Nu, Sigma Pi Sigma, and the American Physical Society.